Chapter 4

Influence of dust on ion cyclotron waves in a two ion plasma

4.1 Introduction

We had, in Chapter 2, considered the influence of dust particles on IC waves, propagating parallel to the magnetic field, in a plasma where the hot ions were described by a bi-Lorentzian or Kappa distribution. The electrons and dust particles were treated as cold. As a starting point of our analysis we had, for simplicity, considered only a single species of ions. However it is well known that, during high - speed flow conditions, the measured proton distributions f_P is well represented by a superposition of two components f_M and f_B; the subscripts M and B referring to the proton main and beam components respectively (Feldman et. al. 1976 a,b; Abraham Shrauner and Feldman, 1977). Some of the observed features of this distribution were: (i) the temperature anisotropy of the main component is large in the sense that the perpendicular temperature $T_{\perp M}$ is $\approx 2.4 T_{\parallel M}$ where the subscripts $\perp$ and $\parallel$ have their usual meaning, (ii) the proton beam generally travels faster than the main component along the magnetic field direction $\vec{B}$, (iii) the number density of the beam component is 20-40 % of the main component and (iv) the temperature T_B of the beam component is 2 - 3 times the main component (Bame et. al., 1975; Abraham

- Shrauner and Feldman, 1977).

We therefore consider, in this Chapter, the influence of dust particles on ion cyclotron waves propagating in a plasma where the hot ions are described by a superposition of two bi-Lorentzians, drifting relative to one another. As in Chapter 2, we find that the dust particles have an appreciable effect on the growth rate of IC waves only when the plasma - β is low. In a low-β plasma the growth rate increases with increasing temperature anisotropy of the hot ions, charge number and density of the dust particles and drift velocity of the drifting component. The growth rate, however, decreases with increasing drifting ion densities. In a high - β plasma, however, the ion cyclotron mode is, in general, damped at the higher frequency end.

4.2 The Dispersion relation

As stated in section 1, the observed proton distributions in the solar wind have been well described as a superposition of two bi-Lorentzian - a main component and a drifting component (Abraham - Shrauner and Feldman, 1977). We denote these components by 'h' and 'd' respectively; in addition 'D' indicates dust and 'e', the electrons. Our ion distribution is thus given by

$$f_P = \frac{1}{\pi^{3/2}} \sum_{h,d} \frac{\Gamma(\kappa+1)}{\kappa^{3/2}\Gamma(\kappa-\frac{1}{2})} \frac{1}{\theta_\perp^2 \theta_\parallel} \left[1 + \frac{v_\perp^2}{\kappa\theta_\perp^2} + \frac{(v_\parallel - v_d)^2}{\kappa\theta_\parallel^2}\right]^{-(\kappa+1)} \tag{4.1}$$

In (1), κ is the spectral index, which for simplicity, we assume to be the same for both the hot and drifting ion components. $\theta_\perp$ and $\theta_\parallel$ (for both the hot and drifting components)

are related to the temperatures respectively perpendicular ($T_{\perp}$) and ($T_{\parallel}$) and mass m by

$$\theta^2_{\perp(\parallel)j} = \left[\frac{\kappa - \frac{3}{2}}{\kappa}\ \frac{2k_B T_{\perp(\parallel)j}}{m}\right] \quad j = h, d \tag{4.2}$$

For the hot proton component $\theta_{\perp h} \neq \theta_{\parallel h}$ but $v_d = 0.0$, while for the drifting proton component $\theta_{\perp h} = \theta_{\parallel h}$ but $v_d \neq 0.0$.

Substituting the derivatives of (1) into the dispersion formula for the left hand polarised ion cyclotron waves (formula (1) of Chapter 2) and carrying out the $dv_{\perp}$ and $dv_{\parallel}$ integrations, we get the dispersion relation for the EMIC waves, propagating parallel to the external magnetic field, as

$$\begin{aligned} c^2k^2 = \omega^2_{ph}\left\{\frac{\omega}{k\theta_{\parallel h}}\left[1 - \frac{kA_p v_c}{\omega}\right]\left[\left(1 + \frac{\zeta_h^2}{\kappa}\right)Z^*_{\kappa}(\zeta_h) + \frac{2\kappa - 1}{2\kappa^2}\zeta_h\right] - A_p\right\} \\ + \omega^2_{pd}\left\{\frac{\omega}{k\theta_d}\left[1 - \frac{kv_d}{\omega}\right]\left[\left(1 + \frac{\zeta_d^2}{\kappa}\right)Z^*_{\kappa}(\zeta_d) + \frac{2\kappa - 1}{2\kappa^2}\zeta_d\right]\right\} \\ - \sum_{j \neq h,d} \omega^2_{pj}\frac{\omega}{\omega - \Omega_j} \end{aligned} \tag{4.3}$$

As in Chapter 2, Z^*_{κ} is the modified plasma dispersion function (Summers and Thorne, 1991) and arises from the $dv_{\parallel}$ integration with arguments

$$\zeta_h = \frac{\omega - \Omega}{k\theta_{\parallel h}} \quad and \quad \zeta_d = \frac{\omega - \Omega - kv_d}{k\theta_d} \tag{4.4}$$

where Ω is the ion gyrofrequency. The definition of the other important terms in (3) are

$$v_c = \frac{\omega - \Omega}{k} \quad and \quad A_p = 1 - \frac{\theta_\perp^2}{\theta_\parallel^2} \tag{4.5}$$

while the other notations are standard.

As a check on (3) we note that when n_d, the density of the drifting ions is equal to zero, (equivalent to $\omega_{pd}^2 = 0$) it reduces to the dispersion relation (4) of Chapter 2. The analyses and discussions that follow closely resemble that in Chapter 2, including neglect of ω^2 in comparison to c^2k^2, and hence we shall give only the most important mathematical steps.

4.3 Low - β case

4.3.1 Dispersion relation

In this section we derive the dispersion relation for EMIC waves when both the ions have a low parallel temperature. Thus the arguments ζ_h and ζ_d of Z_κ^* are $>>1$ and hence we need the asymptotic expansion of the modified plasma dispersion function (relation (7) of Chapter 2). We substitute this into (3) and, as in Chapter 2, neglect ω^2 in comparison to c^2k^2 and also assume that $\omega << \Omega_e$. The charge neutrality condition now is

$$n_h + n_d = z_D n_D + n_e \tag{4.6}$$

with n_j denotes the density of the various components of our plasma. The real part of (3)

on simplification using (6) and rearrangement yields the dispersion relation, which, in final form, can be written as

$$\frac{c^2k^2}{\omega_{ph}^2} = \frac{\left[\frac{x^2}{(1-x)} - \frac{n_d}{n_h}\frac{x^2-(x+1)y}{x-y-1} + \frac{Z_D\frac{n_D}{n_h}x^2}{(x+Z_D\frac{m_i}{m_D})}\right]}{1-\frac{1}{2}\frac{\beta_{\|h}}{(1-x)^2}\left[\frac{x}{(1-x)}+A\right]+\frac{1}{2}\beta_{\|d}\frac{x-y}{(x-y-1)^3}} \tag{4.7}$$

In (7) $y = \frac{kv_d}{\Omega}$ and $x = \frac{\omega}{\Omega}$ $(\omega = \omega_r + i\omega_i)$ while the plasma ion betas are defined as

$$\beta_{\|h} = \frac{8\pi n_h k_B T_{\|h}}{B_o^2} \quad and \quad \beta_{\|d} = \frac{8\pi n_d k_B T_{\|d}}{B_o^2} \tag{4.8}$$

with B_o being the ambient magnetic field.

As a check on (7) we note that for $n_d = 0$ (density of the drifting component = 0), it reduces to relation (10) of Chapter 2.

The expression for the growth/damping can be got from the imaginary part of (3) by substituting the asymptotic expressiones of Z_κ^* into it. The expression for $ImD(x,k)$ is

$$ImD(x,k) = \frac{\Omega\sqrt{\pi}\kappa!}{k\kappa^{3/2}\Gamma(\kappa-\frac{1}{2})}\left\{\frac{1}{\theta_{\|h}}\left[A(1-x)+x\right]\frac{1}{\left(1+\frac{\zeta_h^2}{\kappa}\right)^\kappa} + \frac{n_d}{n_h}\frac{1}{\theta_{\|d}}\left[x-y\right]\frac{1}{\left(1+\frac{\zeta_d^2}{\kappa}\right)^\kappa}\right\} \tag{4.9}$$

while that for the derivative of (7) is

$$\frac{\partial ReD(x,k)}{\partial x} = \frac{x(2-x)}{(1-x)^2} - \frac{n_d}{n_h}\frac{(x-y)(x-y-2)}{(x-y-1)^2} + \frac{z_D\frac{n_D}{n_h}x\left(x+2z_D\frac{m_p}{m_D}\right)}{\left(x+z_D\frac{m_p}{m_D}\right)^2}$$
$$+\frac{c^2k^2}{\omega_{ph}^2}\left\{\frac{\beta_{\|h}}{2}\left[\frac{2A(1-x)+(1+2x)}{(1-x)^4}\right]+\frac{\beta_{\|d}}{2}\left[\frac{1+2x-2y}{(1-x+y)^4}\right]\right\} \quad (4.10)$$

From (9) and (10) we can get the expression for the growth / damping rate as

$$\gamma = \frac{\omega_i}{\Omega} = -\frac{ImD(x,k)}{\frac{\partial ReD(x,k)}{\partial x}} \quad (4.11)$$

Again, as a check on (11), we note that for $n_d = 0$ it reduces to expression (12) of Chapter 2.

However, since the expressions for (7) and (11) are now very complicated due to the additional terms arising from the presence of the drifting protons, no discussion on the lines presented in section 3.2 of Chapter 2 is possible. We shall therefore proceed with the case of high-β plasmas.

4.4 High $\beta_{\|}$ case

4.4.1 The Dispersion relation

As stated above we now extend our derivation to high-β plasmas. When the plasma-β is high we need the small parameter expansion of Z_κ^* (Gomberoff and Vega, 1989); this expansion is given in relation (14) of Chapter 2. Substituting this into the dispersion relation (3) and equating the real part to zero; we find that it can be written as a quadratic equation

$$\left(\frac{c^2\boldsymbol{k}^2}{\omega_{ph}^2}\right)^2 + B\left(\frac{c^2\boldsymbol{k}^2}{\omega_{ph}^2}\right) + C = 0 \tag{4.12}$$

where

$$B = A + \left[1.0 + \frac{n_d}{n_h} - \frac{Z_D n_D}{n_h}\right]x - Z_D^2 \frac{n_D}{n_h}\frac{m_p}{m_D}\frac{x}{x + Z_D\frac{m_p}{m_D}}$$

and

$$C = \frac{2(2\kappa-1)}{2\kappa-3}\left\{\left[\frac{x}{x-1} - A\right]\frac{(x-1)^2}{\beta_{\|h}} + \left(\frac{n_d}{n_h}\right)^2\frac{(x-y)(x-y-1)}{\beta_{\|d}}\right\}$$

The growth rate/damping rate can be calculated from the imaginary part of (3) (with the power series expansion of Z_κ^* substituted in to it) and the derivative of (12).

The final simplified expression can be written as

$$\gamma = \frac{\omega_i}{\Omega} = \frac{p}{q} \tag{4.13}$$

$$p = \frac{\sqrt{\pi}\kappa!}{\kappa^{3/2}\Gamma(\kappa-\frac{1}{2})}\frac{\Omega}{k}\left\{\frac{1}{\theta_{\|h}}\left[A(x-1)+x\right]\frac{1}{(1+\frac{\zeta_\|^2}{\kappa})^\kappa}\right.$$

$$+\frac{n_d}{n_h}\frac{1}{\theta_d}\left[x-y\right]\frac{1}{(1+\frac{\zeta_d^2}{\kappa})^{\kappa}}\Bigg\}$$

and

$$q=\frac{2(2\kappa-1)}{2\kappa-3}\left(\frac{\omega_{ph}^2}{c^2k^2}\right)\left\{\frac{1}{\beta_{\|h}}\left[2A(1-x)+(2x-1)\right]\right.$$

$$\left.+\left(\frac{n_d}{n_h}\right)^2\frac{1}{\beta_d}\left[2x-2y-1\right]\right\}+\left[1+\frac{n_d}{n_h}-Z_D\frac{n_D}{n_h}\right.$$

$$\left.-Z_D^3\frac{n_D}{n_h}\left(\frac{m_p}{m_D}\right)^2\frac{1}{\left(x+Z_D\frac{m_p}{m_D}\right)^2}\right]$$

Again, as a check on our relation (13), we note that for n_d=0, it reduces to relation (19) of Chapter 2.

4.5 Results

In this section we consider the computation for the expressions for the growth rate, namely (11) (low-β case) and (13) (high-β case). We first consider (11) for parameters similar to those of Chapter 2, namely $T_{\|h}=9.0\times10^4$, $B_o=6\times10^{-5}$ Gauss and $n_h=2.8cm^{-3}$. With these parameters $\beta_{\|h}=0.2428$; $\beta_{\|d}$ was calculated from $\beta_{\|h}$ by appropriate conversion. The spectral index κ was kept a constant at 2.

The general parameters for the computations are temperature anisotropy $A = -1.5$, charge number Z_D of the dust = 5000, ratio of the dust to the hot ion density $\frac{n_D}{n_h} = 1.0 \times 10^{-4}$, ratio of the ion to dust mass $\frac{m_p}{m_D} = 1.0 \times 10^{-7}$, ratio of the drifting ion density to the hot ion density $\frac{n_d}{n_h} = 0.5$, the drift velocity normalised to the thermal velocity $\frac{v_d}{\theta_d} = 0.5$ and the ratio of the temperature of the drifting component to the hot component $\frac{T_{\|d}}{T_{\|h}} = 2.0$. Most of these parameters agree well with the standard parameters (Bame et. al.,1975; Abraham - Shrauner and Feldman, 1977).

Figure 1 is a plot of the growth rate γ versus the normalised frequency x. Curve [a] depicts the growth in a single ion plasma ($A = -1.5, n_d = 0, n_D = 0$). We find that the growth rate is small over most of the frequency range; it, however, reaches a maximum at $x \approx 0.475$ and thereafter decreases. Temperature anisotropy is thus the source of instability. Curve [b] depicts the growth rate in a two-ion plasma consisting of a hot and a drifting component ($A = -1.5$, $\frac{n_d}{n_h} = 0.5$, $\frac{v_d}{\theta_d} = 0.5$ and $\frac{T_{\|d}}{T_{\|h}} = 2.0$). We find the growth rate decreases compared to that in a single ion plasma (curve [a]). Curve [c] is for the case which has dust incorporated into the plasma ($\frac{n_D}{n_i} = 1.0 \times 10^{-3}$ and $Z_D = 5000$). We find a large increase in the growth rate as compared to curve [a] with the growth peaking at an earlier frequency.

Figure 2 is again a plot of γ versus x in a plasma with the hot ions, drifting ions ($\frac{n_d}{n_h} = 0.5$, $\frac{v_d}{\theta_d} = 0.5$ and $\frac{T_{\|d}}{T_{\|h}} = 2.0$) and dust ($Z_D = 5000$, $\frac{n_D}{n_h} = 1.0 \times 10^{-4}$ and $\frac{m_p}{m_D} = 1.0 \times 10^{-7}$) as a function of temperature anisotropy of the hot ions. Though the growth rate increases with increasing temperature anisotropy the effect is not as dramatic as inclusion of a small amount of dust (curves [a] and [c] of Figure 1).

Figure 3 is also a plot of γ versus x, but now as a function of the drifting ion density ($\frac{n_d}{n_h}$=0.5, 0.75 and 1.0); the other parameters of the hot ions and dust being the same as in Figure 2. Consistent with the results of Figure 1 we find that the growth rate decreases with increasing ion densities. Figure 4 complements Figure 3 and depicts the variation in the growth rate as a function of the drift velocity of the streaming ions ($\frac{v_d}{\theta_d}$=0.25, 0.5 and 0.75) with $\frac{n_d}{n_h} = 0.5$; the other parameters being the same as in Figure 3. We find that the growth rate is nearly the same at very low frequencies; it, however, increases with increasing $\frac{v_d}{\theta_d}$ at higher frequencies. This result is the familiar two-stream instability; it has already been well studied in a dusty plasma by other workers (Bharuthram et. al.,1992 a & b, Bharuthram, 1997).

Figure 5 is also a plot of γ versus x but as a function of the dust density ($\frac{n_D}{n_h} = 1.0 \times 10^{-5}, 1.0 \times 10^{-4}$ and 1.0×10^{-3}) with Z_D=5000; the parameters for the hot and drifting ions being $A = -1.5$, $\frac{n_d}{n_h} = 0.5$, $\frac{v_d}{\theta_d} = 2.0$ and $\frac{T_{\|d}}{T_{\|h}} = 0.5$. We find that the growth rate is low for low values of dust density and it increases dramatically when the dust density increases beyond a critical value. Figure 6 complements Figure 5 and depicts the growth rate versus frequency as a function of the charge number Z_D of the dust (=1000, 5000 and 10000). The instability increases with increasing Z_D. This is, however, not surprising as the charge number and dust density always occur as a product $Z_D \frac{n_D}{n_h}$.

We next consider the expression for the growth rate in a high-β plasma, namely (13). We use the same value of $\beta_{\|h}$ as in Chapter 2, namely 1.999. As in the low-β case, the common parameters for the figures are $A = -1.5$; for the dust the charge number $Z_D = 5000$, $\frac{m_p}{m_D} = 1.0 \times 10^{-7}$ and $\frac{n_D}{n_h} = 1.0 \times 10^{-2}$; while for the drifting component

$\frac{n_d}{n_h} = 0.5$, $\frac{T_{\|d}}{T_{\|h}} = 2.0$ and $\frac{v_d}{\theta_d} = 0.5$.

Figure 7 is a plot of γ versus x and curve [a] shows the variation of the growth rate in a two component plasma of hot ions and dust ($A = -1.5$, $Z_D = 5000$, $\frac{n_D}{n_i} = 1.0 \times 10^{-2}$ and $\frac{m_i}{m_D} = 1.0 \times 10^{-7}$) while curve [b] is for a plasma that has a drifting component also ($\frac{n_d}{n_h} = 0.5$, $\frac{T_{\|d}}{T_{\|h}} = 2.0$ and $\frac{v_d}{\theta_d} = 0.5$). We find that for the two component plasma the growth rate starts from a large value for low frequencies and decreases steadily with increasing frequency till the wave damps beyond $x = 0.6$. However, the wave growth decreases in a three component plasma containing drifting ions, a result which is consistent with the results in a low - β plasma.

Figure 8 is also a plot of γ versus x as a function of the temperature anisotropy A of the hot ions ($A = -0.5, -1.0$ and -1.5); the other components of the plasma being dust ($Z_D = 5000$, $\frac{m_e}{m_D} = 1.0 \times 10^{-7}$ and $\frac{n_D}{n_i} = 1.0 \times 10^{-2}$ and the drifting component ($\frac{n_d}{n_h} = 0.5$, $\frac{T_{\|d}}{T_{\|h}} = 2.0$ and $\frac{v_d}{\theta_d} = 0.5$). Again, consistent with the results of Figure 2, we find that the growth rate increases with increasing temperature anisotropy of the hot ions.

Figure 9 depicts γ versus x as a function of the charge number Z_D (=1000, 5000 and 10000) with $\frac{m_e}{m_D} = 1.0 \times 10^{-7}$ and $\frac{n_D}{n_i} = 1.0 \times 10^{-2}$. The anisotropy of the hot ions $A = -1.5$ while the parameters of the drifting ions are same as in Figure 8. In contrast to the low-β case we find that, for the high-β situation, the growth rate decreases with increasing charge number. Figure 10 is intended to complement Figure 9 and is a plot of γ versus x as a function of $\frac{n_D}{n_h}$ ($= 1.0 \times 10^{-1}$, $= 1.0 \times 10^{-2}$ and $= 1.0 \times 10^{-3}$) with $Z_D = 5000$ and $\frac{m_e}{m_D} = 1.0 \times 10^{-7}$; the other parameters being the same as in Figure 9. We

find that the growth rate decreases with increasing dust density.

In contrast to the low-β case the growth rate is independent of $\frac{v_d}{\theta_d}$ and similar to Figure 3 the growth rate increases with $\frac{n_D}{n_h}$ but only vary marginally.

4.6 Conclusions

We have, in this Chapter, studied the stability of EMIC waves, propagating parallel to the magnetic field, in a plasma where the two ion components modelled by bi-Lorentzians are drifting relative to one another. The other components that make up the plasma are dust particles and electrons. We find that the growth rate is influenced more strongly by the dust particles than by temperature anisotropy or by drift velocity.

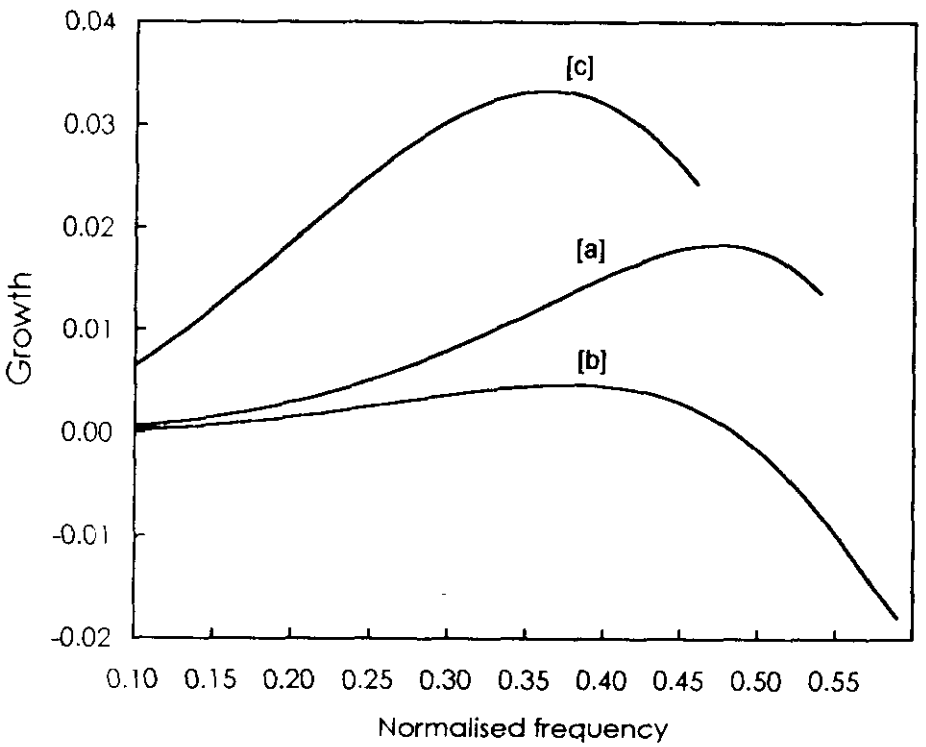

Figure 1: Plot of the growth rate γ versus normalised frequency x. Curve [a] is for a single ion plasma ($\beta_{\parallel th}$=0.2428); curve [b] for a two ion palsma (n_D/n_h = 0.5, v_d/θ_d = 0.5, $T_{\parallel d}/T_{\parallel h}$=2.0) while curve [c] has a third component namely dust (Z_D = 5000 and n_D/n_h = 1.0X10^{-3})

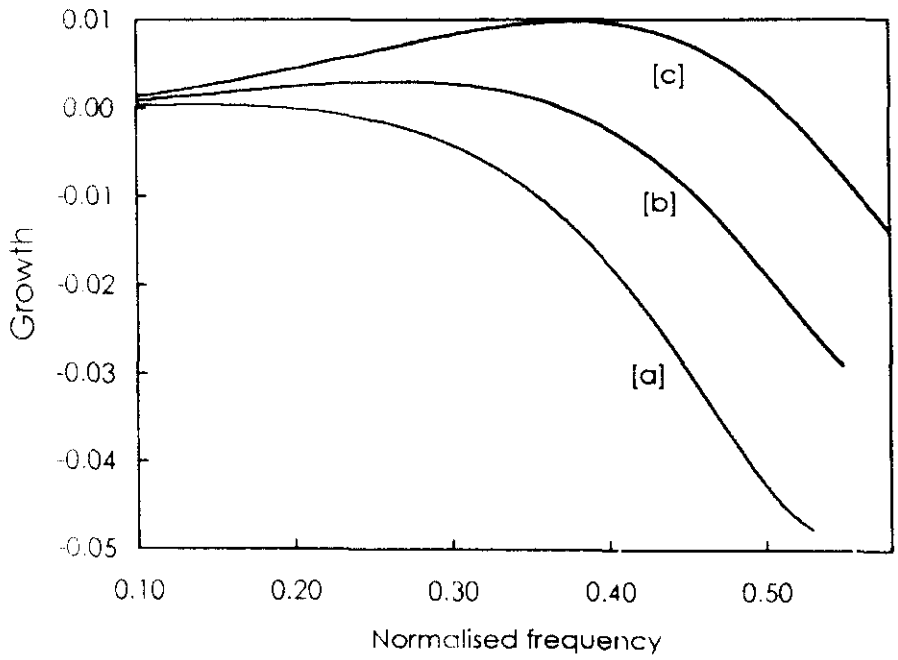

Figure 2: Plot of the growth rate γ versus normalised frequency x as a function of the temperature anisotropy of the hot ions (A=-0.5 (curve[a]), A=-1.0 (curve [b]) and A=-1.5 (curve [c])). The other parameters being, for the drifting component, $n_{+}/n_h = 0.5$. $T_{\|d}/T_{\|h} = 2.0$: for the dust component $Z_D = 5000$ and $n_D/n_h = 1.0X10^{-4}$.

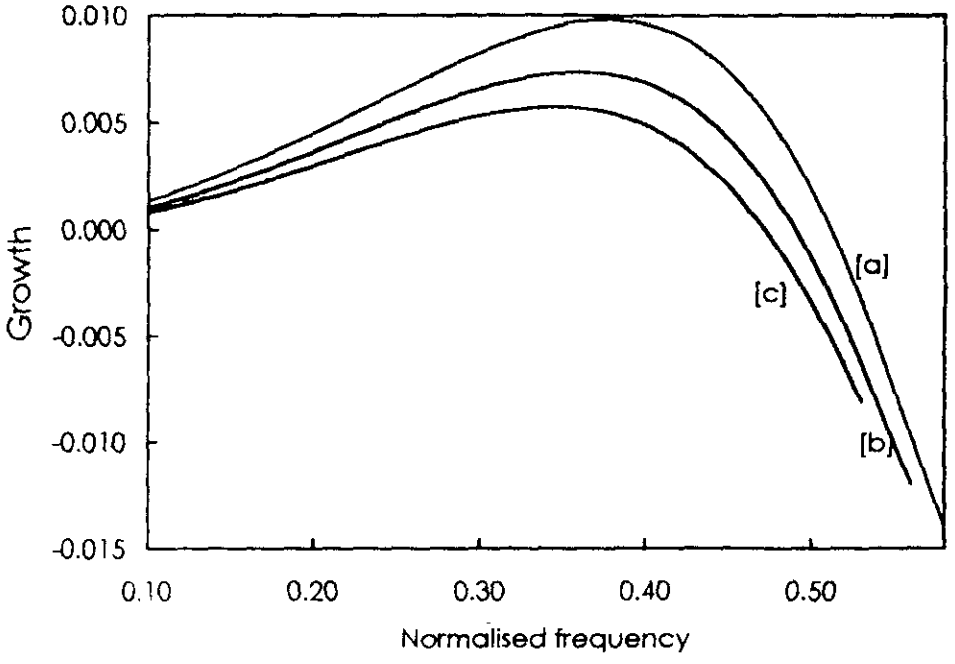

Figure 3: Plot of growth rate γ versus normalised frequency x as a function of the drifting ion density n_d/n_h; curve [a] for n_d/n_h=0.5, curve [b] for n_d/n_h=0.75 and n_d/n_h=1.0 is represented by curve [c], with A = -1.5, the other parameters of the drifting ions and dust being the same as in Figure 2

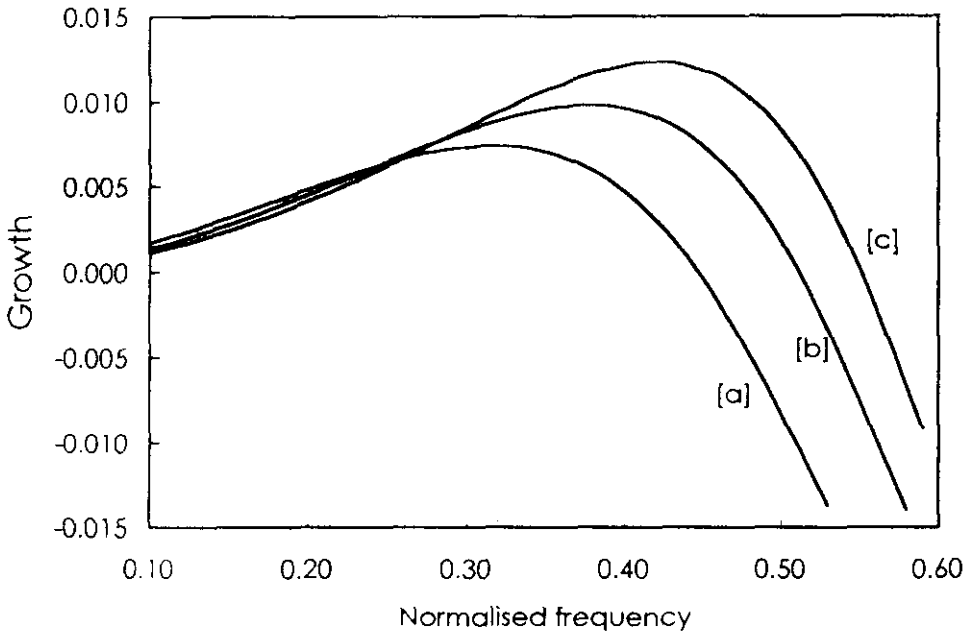

Figure 4: Plot of growth rate versus normalised frequency as a function of v_d/θ_d (curve [a] for 0.25, curve [b] for 0.5 and curve [c] for 0.75) with $n_d/n_h = 0.5$; the other parameters of the hot ions and dust being the same as in Figure 3

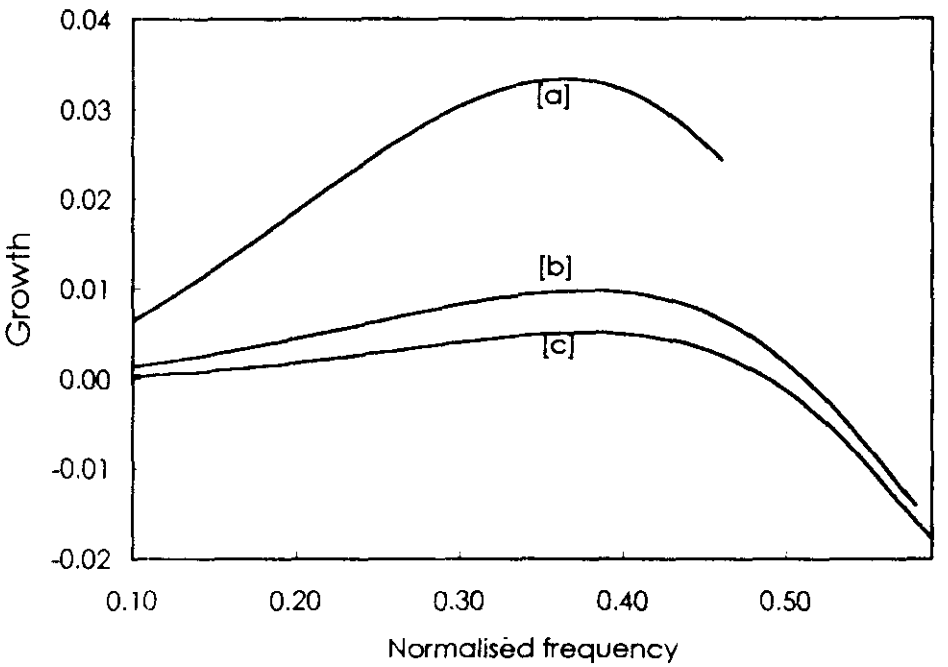

Figure 5: Plot of growth rate versus normalised frequency x as a function of normalised dust density n_D/n_i (=$1X10^{-3}$ for curve [a], $1.0X10^{-4}$ for curve[b] and $1.0X10^{-5}$ for curve [c]) with Z_D = 5000 and m_i/m_D=$1.0X10^{-7}$; the other parameters of the hot and drifting ions being A = -1.5; n_d/n_h=0.5, T_{lld}/T_{llh} = 2.0 and v_d/θ_d = 0.5.

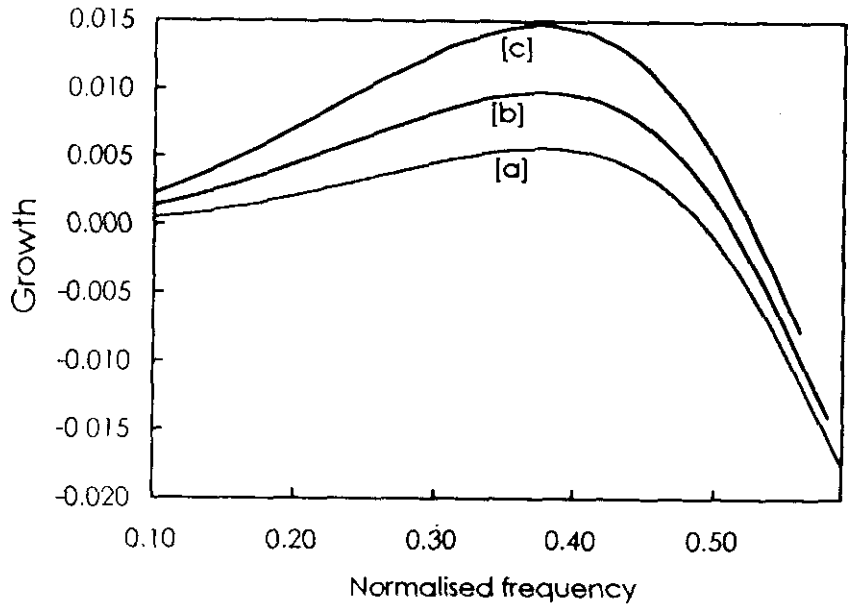

Figure 6: Plot of growth rate γ versus normalised frequency x as a function of Z_D (=1000 (curve [a]), 5000(curve[b]) and 10000 (curve [c])) with density $n_D/n_h = 1.0X10^{-4}$ and mass $m_p/m_D=1.0X10^{-7}$. The parameters of the hot and drifting ions are the same as in Figure 5

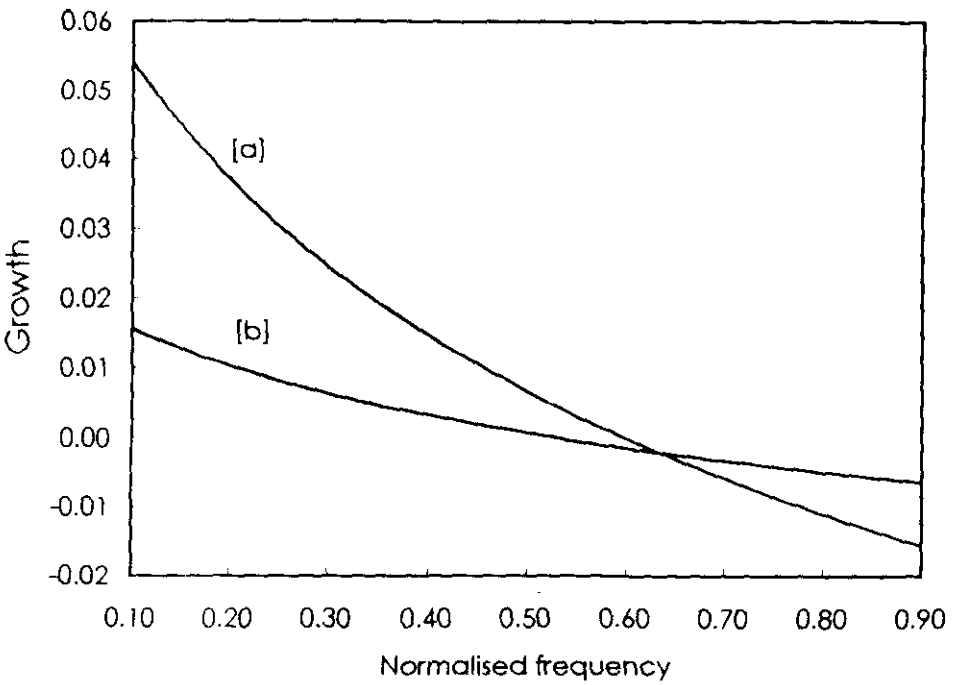

Figure 7: Plot of the growth rate γ versus normalised frequency x in a high-β plasma. Curve [a] is for a plasma containing hot ions (A=-1.5) and dust (Z_D = 5000, n_D/n_h = 1.0X10^{-2} and m_p/m_D = 1.0X10^{-7}) while [b] is for a plasma that has drifting ions also (n_d/n_h = 0.5, T_{lld}/T_{llh} = 2.0 and v_d/v_d = 0.5).

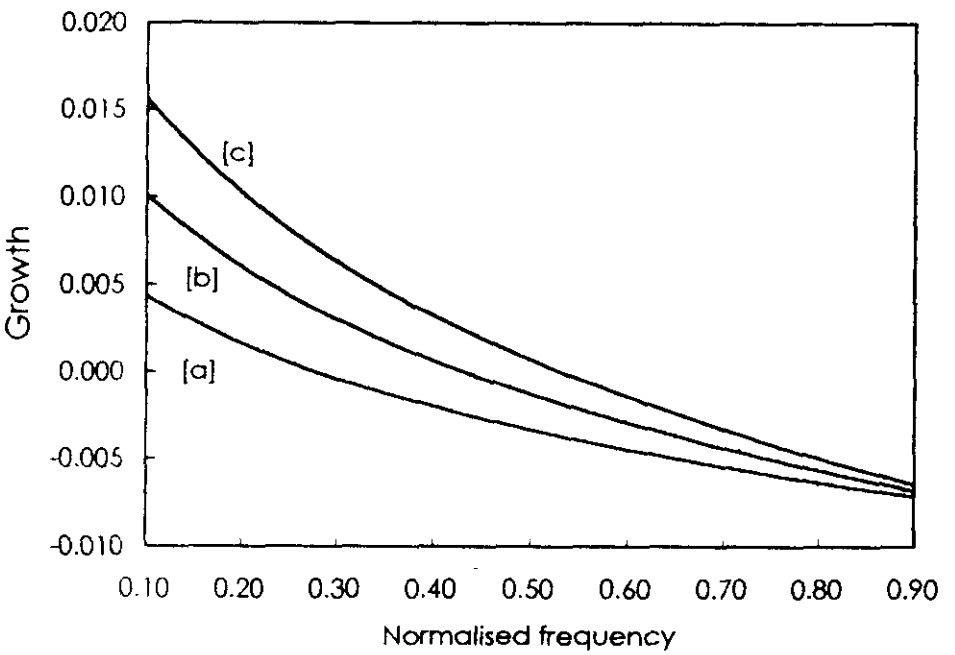

Figure 8: Plot of growth rate γ versus normalised frequency as a function of temperature anisotrpy A of the hot ions (A=-0.5 (curve [a]), -1.0 (curve [b]) and -1.5 (curve [c])), the other components of the plasma being dust (Z_D = 5000, m_p/m_D = 1.0X10^{-7} and n_D/n_i = 1.0X10^{-2}) and drifting ions (n_d/n_h = 0.5, $T_{\|d}/T_{\|h}$ = 2.0 and v_d/θ_d = 0.5)

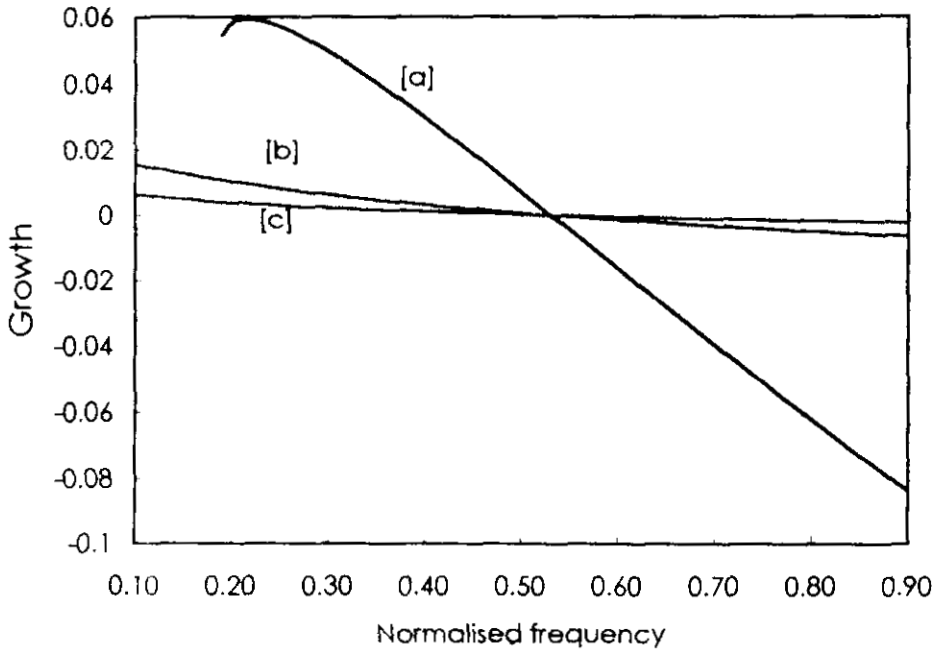

Figure 9: Plot of growth rate γ versus normalised frequency x as a function of Z_D (=1000 (curve [a]), 5000 (curve [b]) and 10000 (curve [c])) with $n_D/n_h = 1.0X10^{-2}$ and $m_p/m_D = 1.0X10^{-7}$ with A = -1.5. The parameters of the drifting ions are the same as in Figure 8

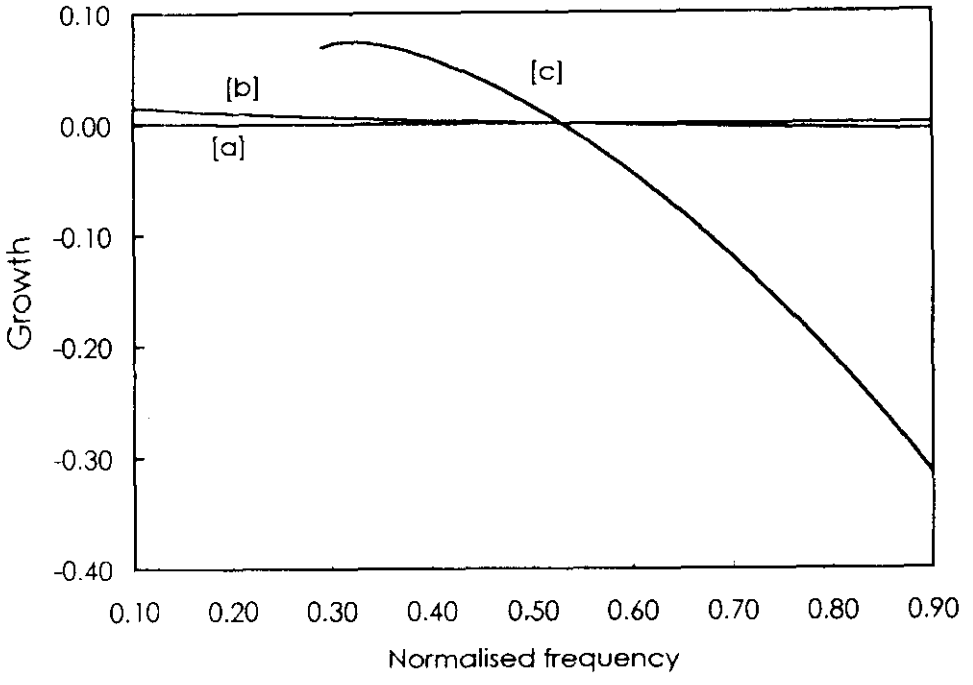

Figure 10: Plot of growth rate γ versus normalised frequency as a function of n_D/n_h (=$1.0X10^{-1}$ (curve [a]), $1.0X10^{-2}$ (curve [b]) and $1.0X10^{-3}$ (curve [c])) with Z_D = 5000 and m_p/m_D = $1.0X10^{-7}$. The parameters for the hot and drifting ions are the same as in Figure 9

4.7 References

Abraham-Shrauner B and Feldman W.C. (1977) J.Geophys. Res.,82,618.

Bame S.J., Asbridge J.R., Fieldman W.C and Montgomery M.D. (1975) Geophys. Res. Lett., 2,373.

Bharuthram R. (1997), Planet. Space Sci., 45, 3379.

Bharuthram R., Saleem H and Shukla P K (1992a), Planet. Space Sci. 40, 973.

Bharuthram R., Saleem H and Shukla P K (1992b), Physica Scripta, 45, 512.

Feldman W.C, Asbridge J.R, Bame S.J, Gary S.P and Montgomery M.D (1976a) J.Geophys. Res.,81,2377.

Feldman W.C, Abraham-Shrauner B., Asbridge J.R and Bame S.J (1976b) Physics of Solar Planetary Environments, edited by D.J.Williams, p.143, AGU, Washington, D.C.

Gomberoff L. and Vega P.(1989) Phys. Cont. Fusion, 31,4 629

Summers D. and Richard M. Thorne (1991) Phys. Fluids B 3, 1835.